



ELSEVIER

Physica D 113 (1998) 172–183

PHYSICA D

The Pauli principle and the vibrational dynamics of protons in solids: A new spin-related symmetry

F. Fillaux¹

Laboratoire de Spectrochimie Infrarouge et Raman, CNRS, 2 rue Henry-Dunant, 94320 Thiais, France

Abstract

Inelastic neutron scattering studies of some hydrogen bonded crystals (e.g., potassium hydrogen carbonate, KHCO_3) have revealed that the dynamics of protons is largely decoupled from the lattice. The KHCO_3 crystal is a prototypical system for proton dynamics which contains centro-symmetric dimer entities $(\text{HCO}_3^-)_2$ linked by moderately strong hydrogen bonds. The quantum dynamics of pairs of coupled oscillators is analyzed. It is shown that the Pauli principle applied to normal coordinates for fermions gives new quantum properties in the degenerate ground state. Vibrational wave functions for the singlet and triplet states are derived. A new spin-related selection rule is proposed: the dynamics of fermions (e.g., H atoms) is decoupled from the dynamics of bosons (e.g., C and O atoms). Scattering functions for the protons are calculated with various models: the single harmonic oscillator, the double minimum potential and pairs of coupled harmonic oscillators. It is concluded that quantum interferences should be observed with elastic neutron scattering for pairs of coupled fermions. Copyright © 1998 Elsevier Science B.V.

Keywords: Neutron scattering; Hydrogen bond; Proton transfer; Pauli principle

1. Introduction

Nowadays, incoherent inelastic neutron scattering (INS) spectra, obtained over a rather large energy transfer range (e.g., from ~ 0 to 4000 cm^{-1} with the TFXA spectrometer at the ISIS pulsed neutron-source, Rutherford, Appleton Laboratory, UK), provide information on the vibrational dynamics in solids that cannot be obtained with the more conventional optical techniques (infrared and Raman). Although the INS technique is rather young, it has already had a spectacular impact on two central problems of vibrational spectroscopy: the relevance of normal modes to represent vibrational spectra and the quantum transfer of protons within double minimum potentials [1].

It is widely accepted that vibrational dynamics of atoms and molecules is reasonably well represented with harmonic force-fields. Within this framework, the resolution of the secular equation transforms a set of (say N) coupled oscillators into (N) independent oscillators along orthogonal (normal) coordinates. Eigenvalues are the normal frequencies and eigenvectors give atomic displacements for each normal mode [2]. These vectors are related

¹ Fax: (1) 49781323.

to the band intensities. Unfortunately, transition moment operators for optical spectra (namely the derivatives of the dipole moment in the infrared and those of the polarizability tensor in Raman) are largely unknown. These quantities cannot be measured independently of the optical spectra, and accurate calculation is still beyond theoretical approaches (e.g., quantum chemistry). Therefore, band intensities measured with the optical techniques cannot be fully exploited, and force-fields refined with only the observed frequencies are largely underdetermined. For complex systems, symmetry considerations or/and isotopic substitution may remove only partially this underdetermination.

With INS, intensities can be calculated more rigorously. For each normal mode, the band intensity is proportional to the mean-square amplitudes of the atomic displacements (given by the eigenvector) scaled by the nuclear cross-sections [3–8]. Force-fields can be thus refined with respect to the full spectral profiles including both frequencies and intensities [9]. The incoherent scattering cross-section for protons being about one order of magnitude greater than for any other atom, this technique is most powerful for hydrogenous samples. Intensities are dominated by modes involving large proton displacements, and contributions from other atoms are difficult to estimate precisely.

Another great advantage of INS compared to optical techniques is that spectra can be measured over a range of momentum transfer ($\mathbf{Q} = \mathbf{k}_i - \mathbf{k}_f$ with $|\mathbf{k}_i| = 2\pi/\lambda_i$ and $|\mathbf{k}_f| = 2\pi/\lambda_f$, where λ_i and λ_f are the incident and scattered wavelengths, respectively). The scattering process can be represented with the scattering function [8]:

$$S(\mathbf{Q}, \omega) = |\langle \Psi_f(\mathbf{r}) | \exp(i\mathbf{Q} \cdot \mathbf{r}) | \Psi_i(\mathbf{r}) \rangle|^2 \delta(E_{if} - \hbar\omega), \quad (1)$$

where $\Psi_i(\mathbf{r})$ and $\Psi_f(\mathbf{r})$ are the wave functions in the initial and final states, respectively. E_{if} is the energy of the transition and $\hbar\omega$ is the neutron energy transfer. For each vibrational mode, the INS spectral profile in \mathbf{Q} is the Fourier transform of the autocorrelation function $|\Psi_i\Psi_f|$ that contains spatial information on the wave functions.

In molecular crystals, when harmonic force-fields are used to represent local atom–atom interactions, the mean positions of the protons that oscillate at high frequency (internal modes) follow adiabatically the slow lattice vibrations (usually referred to as external modes in this context) corresponding to translational and librational motions of the molecular entities. This riding effect gives rise to large intensities for the modes at low frequency. Moreover, the intensity of the internal molecular vibrations is multiplied by an exponential term ($\exp[-\langle (\mathbf{Q} \cdot \mathbf{u})^2 \rangle]$, where \mathbf{u} is the displacement vector for the atoms) referred to as the Debye–Waller factor. This term should depress dramatically the internal mode intensities at high momentum transfer values. It has been speculated that for many molecular crystals internal modes above $\sim 1000 \text{ cm}^{-1}$ should be almost invisible with INS. However, this is largely in error. For example, bands due to CH stretching modes were observed at $\sim 3000 \text{ cm}^{-1}$, and the role of the Debye–Waller factor had to be reconsidered [4–7].

More recently, it has been shown that the INS spectrum of potassium hydrogen carbonate (KHCO_3) cannot be represented with conventional harmonic force-fields [10]. The observed intensity of the lattice modes at low frequency is smaller than the calculated one by at least one order of magnitude. It was concluded that there is virtually no riding effect. The protons are almost totally decoupled from the surrounding heavy atoms and their dynamics is better represented with localized modes in a “fixed” (laboratory) referential frame. From the standpoint of INS spectra, KHCO_3 can be regarded as a crystal of protons so weakly coupled to the surrounding atoms that the framework of carbonate and K^+ ions can be ignored.

Dynamical models are thus greatly simplified. Besides, this view is not specific to the ionic nature of the crystal. Similar conclusions were obtained with molecular crystals such as the N-methylacetamide molecule [11] and polyglycine [12]. These results severely undermine the representation of vibrational spectra with usual normal modes. However, the phenomenological approach proposed so far lacks contact with physics. A major aim of this work is to account for these observations within a more firmly based theoretical framework. It is shown that the decoupling of the proton modes from the lattice could be a consequence of the Pauli principle.

Another highlight of the INS technique concerns the proton transfer along pre-existing hydrogen bonds. This is one of the simplest chemical reactions which is of great importance in many fields in physics, chemistry and

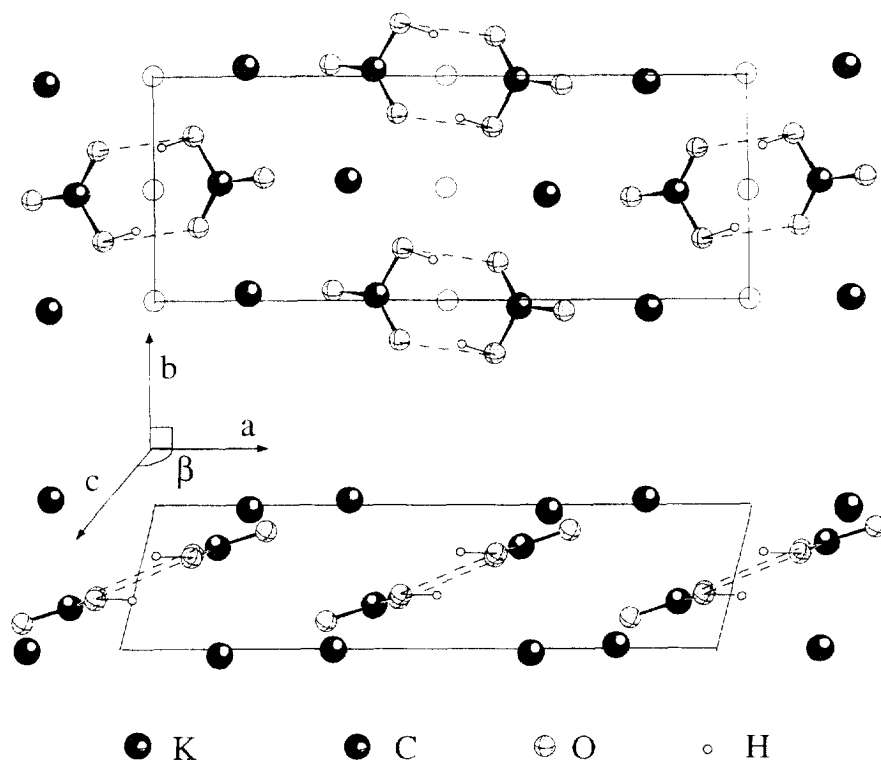


Fig. 1. Schematic view of the crystalline structure of KHCO_3 after [4].

biology [13–18]. KHCO_3 is a prototypical system for proton transfer dynamics [10,19,20]. The crystal contains centro-symmetric dimer entities $(\text{HCO}_3^-)_2$ (Fig. 1), and this structure remains unchanged from 298 to 98 K [21,22]. (We are not aware of any diffraction work at a lower temperature.) The hydrogen bond with length $\text{O} \cdots \text{O} = 2.59 \text{ \AA}$ is moderately strong [23]. At 298 K protons are disordered between two sites located at $\pm 0.3 \text{ \AA}$ off-center of the hydrogen bond, with population ratio of $\sim 1 : 4$.

Diffraction studies cannot distinguish statistical disorder from dynamical disorder. Only the vibrational spectroscopy probes dynamics on a timescale at which quantum proton transfer (tunneling) may occur. Furthermore, tunneling is best observed for vibrations along the reaction path. In this context, the OH-stretching vibration in KHCO_3 is of particular interest. In the infrared and Raman this mode gives broad bands, with several sub-maxima between 1800 and 3500 cm^{-1} [24–26]. Different models have been proposed for the dynamics of the hydrogen bond, and extensive quantum-mechanical calculations have been performed [13,14,23]. Unfortunately, a detailed understanding of the various band shaping mechanisms is still lacking. In spite of these limitations, a quasi-symmetric double minimum potential along the proton stretching mode coordinate was proposed [19]. The “tunneling” transition associated with quantum transfer of a single proton was calculated at 213 cm^{-1} , and was observed later on at 216 cm^{-1} [10], thanks to the great sensitivity of the INS technique to proton displacements with large amplitudes. The dynamical nature of the proton disorder was thus established. Surprisingly, the “tunneling” band is rather sharp. On the one hand, this confirms that the proton transfer is totally decoupled from the heavy atom dynamics, in line with the remainder of the spectrum. On the other hand, this is in contrast to the “phonon assisted tunneling” model [17] that supposes a large modulation of the double minimum potential by the $(\text{O} \cdots \text{O})$ low frequency modes of the hydrogen bond. Tunneling transitions observed in various hydrogen bonds are quite similar [27]. Clearly, the

opportunity to observe tunneling transitions with INS is an important step forward for a better understanding of the proton transfer dynamics.

In order to rationalize the peculiar dynamics of protons, simple models are revisited. The dynamics of pairs of coupled oscillators is presented in Section 2. It is shown that the usual representation with normal coordinates is relevant only for bosons. For fermions, the Pauli principle yields quantum corrections to the usual normal mode analysis in the ground state. The separation of the dynamics for fermions and bosons is discussed in Section 3. The scattering functions for single oscillators with harmonic or double minimum potentials and for pairs of coupled oscillators are given in Section 4. The spin correlation for pairs of fermions gives quantum interference that could be observed with elastic neutron scattering.

2. Pairs of coupled oscillators

In the KHCO_3 crystal, intra- and inter-dimer coupling terms can be distinguished with the optical and INS techniques. The intra-dimer terms give band splitting into B_u and A_g symmetry species observed in the infrared and with Raman, respectively [24–26]. The splitting is quite different for the three modes: ~ 200 , 60 and 40 cm^{-1} for the stretching, in-plane and out-of-plane bending, respectively. The inter-dimer coupling terms, on the other hand, yield the density-of-states that are probed with INS. However, the observed band widths for the proton modes are similar with the three techniques. Consequently, inter-dimer coupling terms are rather weak. In this paper, inter-dimer interactions are ignored.

The dynamics of a centro-symmetric pair of protons can be represented with two identical harmonic oscillators with mass m moving along collinear coordinates x_1 , x_2 , and coupled to one another (Fig. 2). The Hamiltonian is [28]:

$$H = \frac{1}{2m}(P_1^2 + P_2^2) + \frac{1}{2}m\omega_{0x}^2[(x_1 - X_0)^2 + (x_2 + X_0)^2 + 2\lambda_x(x_1 - x_2)^2], \quad (2)$$

P_1 and P_2 are the kinetic momenta. The harmonic frequency of the uncoupled oscillators at equilibrium positions $\pm X_0$ is ω_{0x} . The coupling potential proportional to λ_x depends only on the distance between the two pendula. The equilibrium positions of the coupled oscillators are at $\pm X'_0 = \pm X_0/(1 + 4\lambda_x)$.

2.1. Normal coordinates

Complex vibrations of a system of coupled harmonic oscillators can be expressed as linear combinations of normal modes. In the simple case of Eq. (2), normal coordinates are the symmetric (x_s) and antisymmetric (x_a) displacements of the two particles. These coordinates are not totally determined by the secular equation and can be defined proportional to an arbitrary factor (say K) that determines the norm of the normal coordinates and the effective mass of the normal modes. Because the effective oscillator mass of the normal mode is a non-physical

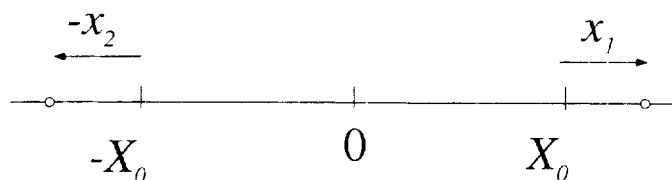


Fig. 2. Schematic representation of two identical harmonic oscillators.

parameter that cannot be measured, frequencies and wave functions are independent of K . For the sake of simplicity, it is convenient to use normalized coordinates corresponding to an effective mass of m for each mode:

$$x_a = \frac{1}{\sqrt{2}}(x_1 + x_2), \quad x_s = \frac{1}{\sqrt{2}}(x_1 - x_2), \quad P_a = \frac{1}{\sqrt{2}}(P_1 + P_2), \quad P_s = \frac{1}{\sqrt{2}}(P_1 - P_2). \quad (3)$$

Substitution in Eq. (2) gives the desired separation of the normal modes:

$$H = \left\{ \frac{P_a^2}{2m} + \frac{1}{2}m\omega_{0a}^2 x_a^2 \right\} + \left\{ \frac{P_s^2}{2m} + \frac{1}{2}m\omega_{0s}^2 (1 + 4\lambda_x) |x_s - \sqrt{2}X'_0|^2 \right\} + m\omega_{0s}^2 X_0^2 \frac{4\lambda_x}{1 + 4\lambda_x}. \quad (4)$$

The normal frequencies are then

$$\omega_a = \omega_{0a} \quad \text{and} \quad \omega_s = \omega_{0s} \sqrt{1 + 4\lambda_x}. \quad (5)$$

For quantum systems quantization applied to normal coordinates gives [28]

$$\Psi_{nm} = \Psi_{am}(x_a) \times \Psi_{sn}(x_s - \sqrt{2}X'_0), \quad \text{and} \quad E_{nm} = (am + \frac{1}{2})\hbar\omega_a + (sn + \frac{1}{2})\hbar\omega_s. \quad (6)$$

2.2. Spin–spin correlation in the ground state

In the normal mode analysis presented above, there is no assumption on the nature (fermions or bosons) of the quantum particles under investigation. However, because the ground state is degenerate, quantum effects are different for fermions and bosons. Eq. (6) is relevant only for bosons. For fermions, according to the Pauli principle, the total wave function including spins is antisymmetrical with respect to particle permutation. Consequently, the spins of the two protons are correlated in a singlet ($S = 0$) and a triplet ($S = 1$) state. The spatial part of the wave function is symmetrical with respect to particle permutation in the singlet state and antisymmetrical in the triplet state. This can be written as

$$\begin{aligned} \Theta_{0\pm}(x_1, x_2) = & \frac{1}{\sqrt{2}} \{ \Psi_{a0}[(x_1 - X'_0) + (x_2 + X'_0)] \Psi_{s0}[(x_1 - X'_0) - (x_2 + X'_0)] \\ & \pm \Psi_{a0}[(x_2 - X'_0) + (x_1 + X'_0)] \Psi_{s0}[(x_2 - X'_0) - (x_1 + X'_0)] \} \end{aligned} \quad (7)$$

or

$$\Theta_{0\pm}(x_1, x_2) = \frac{1}{\sqrt{2}} \Psi_{a0}(x_a) [\Psi_{s0}(x_s - \sqrt{2}X'_0) \pm \Psi_{s0}(x_s + \sqrt{2}X'_0)]. \quad (8)$$

The spin interaction and the exchange integral for protons separated by several Å are negligible. Therefore, the energy splitting for the singlet and triplet states can be ignored. The ground state remains degenerate as for the bosons. The consequence of the Pauli principle is merely to impose the symmetry.

3. Vibrational coupling

In a real crystal, within the harmonic force-field approach, the hydrogen atoms oscillate in local potentials defined with respect to the surrounding atoms (lattice referential). For example, in the KHCO_3 crystal, protons are engaged in hydrogen bonds between two carbonate entities (CO_3^{2-}) forming centro-symmetric dimers. If there is no coupling between the protons and the dimer oscillations, the dynamics is represented with symmetric and antisymmetric

normal coordinates for proton modes (x_s, x_a) and for dimer modes (X_s, X_a). If the nuclear spins are ignored, the wave function analogous to Eq. (6) is

$$\Xi_0(x_1, x_2, X_1, X_2) = \Psi_{a0}(x_a)\Psi_{s0}(x_s - \sqrt{2}X'_0F)\Phi_{a0}(X_a)\Phi_{s0}(X_s - \sqrt{2}X''_0). \quad (9)$$

Alternatively, if the nuclear spins are considered, the total vibrational wave function in the degenerate ground state is antisymmetrical with respect to proton permutation according to the Pauli principle, and it is unaffected by the permutation of the (CO_3^{2-}) entities (the carbon and oxygen atoms are bosons). The wave function analogous to Eq. (8) is

$$\begin{aligned} \Xi_{0\pm}(x_1, x_2, X_1, X_2) = & \frac{1}{\sqrt{2}}\Psi_{a0}(x_a)[\Psi_{s0}(x_s - \sqrt{2}X'_0) \pm \Psi_{s0}(x_s + \sqrt{2}X'_0)] \\ & \times \Phi_{a0}(X_a)\Phi_{s0}(X_s - \sqrt{2}X''_0). \end{aligned} \quad (10)$$

Alternatively, if the proton and dimer modes are coupled via off diagonal elements in the dynamical matrix, the normal coordinates (ξ_i) are linear combinations of the proton and carbonate coordinates. It is no longer relevant to distinguish fermions and bosons, and it is no longer possible to define antisymmetrized wave functions analogous to Eq. (9). This yields a conflict with the Pauli principle since the two protons are still indistinguishable in the degenerate ground state.

Clearly, there are two mutually exclusive approaches. First, the dynamics is represented with normal coordinates mixing fermion and boson displacements. This is the usual approach in vibrational spectroscopy but this is in conflict with the Pauli principle. Second, the Pauli principle imposes that there is no mixing of the normal coordinates for fermions, on the one hand, and bosons, on the other. In this latter case, off diagonal elements mixing fermion and boson displacements are forbidden and the total wave function is strictly factored as

$$\Psi(\dots x_f \dots, \dots X_b \dots) = \psi(\dots x_f \dots)\varphi(\dots X_b \dots), \quad (11)$$

where x_f and X_b are coordinates for the fermions and bosons, respectively.

We conclude that the decoupled dynamics of the proton and lattice modes corresponding to boson displacements (C and O atom) is a consequence of the Pauli principle. Because this decoupling has been observed for quite different systems, it is not likely due to accidental cancellation of the relevant off diagonal elements. Moreover, because the spin interaction is extremely weak, the factorization of the wave function must be regarded as a spin-related selection rule. This rule applies to pairs of coupled protons, irrespective of the magnitude of the coupling term and of the mean distance between their equilibrium positions. This separation of the fermion and boson dynamics is supposed to be the fundamental justification of the localized proton modes introduced empirically to account for previous observations [10–12]. It may also account for the observation of well-defined bands at high energy and momentum transfer values [4–7] and narrow bands for tunneling transitions [10,27], in conflict with the phonon assisted model [17].

The Pauli principle applies only to the degenerate ground state. The excited vibrational states have no degeneracy and the dynamics should be represented with the usual normal modes including all atomic coordinates, irrespective of their nuclear spins. Coupling between fermions and bosons are effectively observed on vibrational spectra (e.g., between the OH in-plane bending and the stretching of the carbonate ions in KHCO_3 [10]). Therefore, the normal coordinates could be different in the ground and excited states. The calculation of the scattering function should be more complex than with the usual normal mode analysis.

4. Scattering functions

The spin-related selection rule presented above could be of great importance for vibrational spectroscopy. Therefore, this rule needs support from experiments. In this part, it is shown that the spin correlation can be evidenced with elastic neutron scattering measurements. In order to establish the specific fingerprint of the spin correlation, the scattering functions for the linear harmonic oscillator, for the double minimum function and for pairs of coupled oscillators are calculated.

4.1. Harmonic potential

The wave functions for an isolated linear harmonic oscillator along the x coordinate are [8]

$$\Psi_n(x) = \left(\frac{a_x^2}{\pi}\right)^{1/4} \frac{1}{\sqrt{2^n n!}} H_n(a_x x) \exp\left(-\frac{1}{2}a_x^2 x^2\right) \quad (12)$$

with

$$a_x^2 = \frac{m\omega_{0x}}{\hbar} = \frac{1}{2u_{0x}^2}, \quad (13)$$

H_n is the Hermite polynomial of degree n , m is the oscillator mass and u_{0x}^2 is the mean-square amplitude in the ground state. The elastic scattering function according to Eq. (1) is

$$S(Q_x, \omega) = \exp(-Q_x^2 u_{0x}^2) \delta(\omega). \quad (14)$$

The Gaussian profile is centered at $Q_x = 0$ (see Fig. 3).

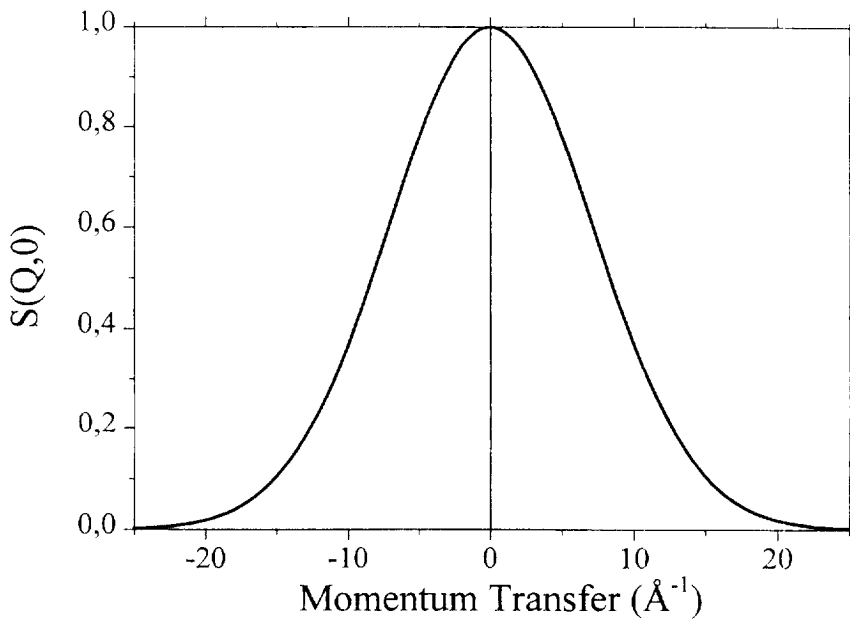


Fig. 3. Theoretical profile for elastic neutron scattering by a single harmonic oscillator, according to Eq. (14) with $n = 0$ and $u_{0x}^2 = 10^{-2} \text{Å}^2$.

4.2. Double minimum potential

For a single particle in a symmetrical double minimum potential the ground state splits into two sublevels, symmetric (0^+) and antisymmetric (0^-), respectively. $E_{0^-} - E_{0^+} = \hbar\omega_{0^-}$ is the tunnel splitting. If the potential barrier is sufficiently high, convenient approximations of the wave functions for these states are symmetrical and antisymmetrical combinations of harmonic wave functions centered at the potential minima $\pm X_0$:

$$\Psi_{0^\pm}(x) = \frac{1}{\sqrt{2[1 \pm \exp(-a_x^2 X_0^2)]}} |\Psi_0(x - X_0) \pm \Psi_0(x + X_0)| \quad (15)$$

and the scattering functions analogous to Eq. (1) are

$$\begin{aligned} S(Q_x, \omega)_{0^+0^+} &= \frac{1}{1 + \exp(-X_0^2/2u_{0x}^2)} \left| \left[\cos(Q_x X_0) + \exp\left(-\frac{X_0^2}{2u_{0x}^2}\right) \right] \exp\left(-\frac{Q_x^2 u_{0x}^2}{2}\right) \right|^2 \delta(\omega), \\ S(Q_x, \omega)_{0^+0^\mp} &= \frac{1}{\sqrt{1 - \exp(-X_0^2/u_{0x}^2)}} \left| i \sin(Q_x X_0) \exp\left(-\frac{Q_x^2 u_{0x}^2}{2}\right) \right|^2 \delta(\omega_{0^-} \pm \omega), \\ S(Q_x, \omega)_{0^-0^-} &= \frac{1}{1 - \exp(-X_0^2/2u_{0x}^2)} \left| \left[\cos(Q_x X_0) - \exp\left(-\frac{X_0^2}{2u_{0x}^2}\right) \right] \exp\left(-\frac{Q_x^2 u_{0x}^2}{2}\right) \right|^2 \delta(\omega). \end{aligned} \quad (16)$$

The periodical terms account for interferences between waves scattered by the same proton at the two sites. The exponential terms between brackets stem from the overlap of the wave functions centered at X_0 and $-X_0$, respectively. They rapidly become negligible for large X_0 values. $S_{0^+0^+}$ and $S_{0^-0^-}$ give interferences analogous to the optical fringes observed with two slits separated by $2X_0$ and whose widths are u_{0x}^2 (see Fig. 4(A)). These interferences can be observed only at a low temperature ($kT \ll \hbar\omega_{0^-}$) and with sufficient energy resolution. $S_{0^+0^-}$ and $S_{0^-0^+}$ give complementary interference fringes for the tunneling transition at $\hbar\omega_{0^-}$ (see Fig. 4(B)). This corresponds to inelastic scattering. However, if the tunnel splitting is smaller than the energy resolution, $S_{0^\pm 0^\pm}$ and $S_{0^\mp 0^\mp}$ are measured simultaneously and the summation of the $\sin^2(Q_x X_0)$ and $\cos^2(Q_x X_0)$ terms gives a spectrum very similar to, and practically indistinguishable from that of a harmonic oscillator (see Fig. 4(C)).

4.3. Pair of coupled oscillators (bosons)

With the wave function given in Eq. (6), the elastic incoherent scattering function:

$$\begin{aligned} S(Q_x, \omega) &= \{ |\langle \Psi_{s0}(x_s - \sqrt{2}X'_0) \Psi_{a0}(x_a) | \exp(iQ_x x_1) | \Psi_{s0}(x_s - \sqrt{2}X'_0) \Psi_{a0}(x_a) \rangle|^2 \\ &\quad + |\langle \Psi_{s0}(x_s - \sqrt{2}X'_0) \Psi_{a0}(x_a) | \exp(iQ_x x_2) | \Psi_{s0}(x_s - \sqrt{2}X'_0) \Psi_{a0}(x_a) \rangle|^2 \} \delta(\omega) \end{aligned} \quad (17)$$

gives

$$S(Q_x, \omega) = 2 \exp \left[-Q_x^2 \left(\frac{u_{0x}^2}{2\sqrt{1+4\lambda_x}} + \frac{u_{0x}^2}{2} \right) \right] \delta(\omega). \quad (18)$$

The Gaussian profile is equivalent to that for the isolated harmonic oscillator in Eq. (14) with a mean-square amplitude of $\approx u_{0x}^2(1 - \lambda_x)$. Practically, it is impossible to distinguish coupled pairs of bosons and isolated oscillators.

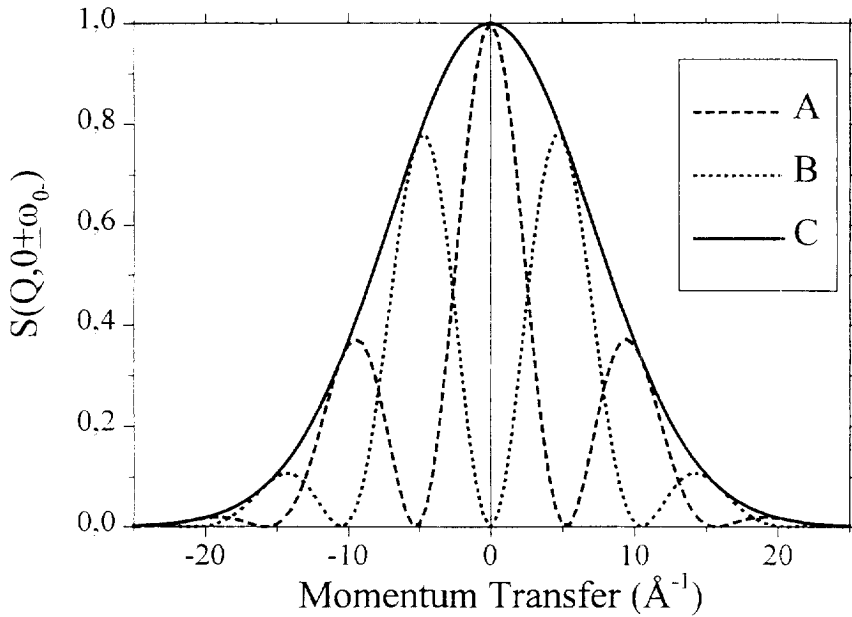


Fig. 4. Theoretical profile for neutron scattering by a proton in a double minimum potential function, according to Eq. (16) With $\mu_{0v}^2 = 10^{-2} \text{ \AA}^2$ and $X_0 = 0.3 \text{ \AA}$: (A) $S_{0^+0^-} \approx S_{0^-0^+}$; (B) $S_{0^+0^-} = S_{0^-0^+}$ and (C) total scattering function.

4.4. Pair of coupled oscillators (fermions)

The spin correlation gives interferences between the waves scattered by the two particles. The singlet and triplet states compare to the para and ortho species of the hydrogen molecule [8]. For this molecule, the vibrational ground state depends only on the symmetric stretching. The antisymmetric motion corresponds to the translation of the free molecule. The vibrational wave functions are

$$\Theta_{0\pm}(x_1, x_2) = \frac{1}{\sqrt{2}} [\Psi_{s0}(x_1 - x_2 - R_0) \pm \Psi_{s0}(x_1 - x_2 + R_0)]. \quad (19)$$

R_0 is the bond length. The part of the scattering function depending on the spatial coordinates is

$$S(Q_x, \omega) = |\langle \Theta_{0\pm}(x_1, x_2) | \exp iQ_x x_1 \pm \exp iQ_x x_2 | \Theta_{0\pm}(x_1, x_2) \rangle|^2 \delta(\omega). \quad (20)$$

The scattering function is similar to Eq. (16) for the double minimum potential, apart from the term $S_{0\pm 0\pm}$ since the para and ortho states correspond to different molecular species. Therefore, the interference can be observed with elastic scattering. The scattered intensity is determined by the matrix elements $|\langle I' | \hat{b}_1 \pm \hat{b}_2 | I \rangle|^2$, where I and I' are the total nuclear spins for the initial and final states, respectively, whilst \hat{b}_1 and \hat{b}_2 are the scattering amplitude operators for nuclei 1 and 2 [8]. The matrix elements are

$$0+ \rightarrow 0+: \frac{\sigma_c}{\pi} \quad \text{and} \quad 0- \rightarrow 0-: \frac{\sigma_c}{\pi} + \frac{2}{3} \frac{\sigma_i}{\pi}, \quad (21)$$

where $\sigma_c = 4\pi |\bar{b}|^2$ and $\sigma_i = 4\pi (|\bar{b}|^2 - |\bar{b}|^2)$ are the coherent and incoherent scattering cross-sections of the hydrogen atom.

In the hydrogen molecule, interference occurs because it is not possible to distinguish scattering by atom 1 at site 1 or atom 2 at site 2. Similar interference should be observed for the coupled oscillators in KHCO_3 . Furthermore,

the singlet and triplet states do not correspond to different molecular species. Consequently, it is no longer possible to assign the operator \hat{b}_1 to atom 1 and the operator \hat{b}_2 to atom 2. Interference due to the spin correlation combines with interference due to the fact that the operator \hat{b}_1 can be at site 1 or 2 and the operator \hat{b}_2 at site 2 or 1. The corresponding scattering functions are

$$S(Q_x, \omega) = |\langle \Xi_{0\pm} | \exp i Q_x (x_1 - X'_0) \pm \exp i Q_x (x_1 + X'_0) | \Xi_{0\pm} \rangle|^2 + |\langle \Xi_{0\pm} | \exp i Q_x (x_2 - X'_0) \pm \exp i Q_x (x_2 + X'_0) | \Xi_{0\pm} \rangle|^2 \delta(\omega) \quad (22)$$

or

$$S(Q_x, \omega)_{0^+0^-} = 2 \cos^2(Q_x X'_0) \left[\cos(Q_x X'_0) + \exp\left(-\frac{X'^2_0}{2u^2_{0x}}\right) \right]^2 \exp -Q_x^2 \left(\frac{u^2_{0x}}{2\sqrt{1+4\lambda_x}} + \frac{u^2_{0x}}{2} \right) \delta(\omega),$$

$$S(Q_x, \omega)_{0^+0^+} = 2 \sin^4(Q_x X'_0) \exp -Q_x^2 \left(\frac{u^2_{0x}}{2\sqrt{1+4\lambda_x}} + \frac{u^2_{0x}}{2} \right) \delta(\omega), \quad (23)$$

$$S(Q_x, \omega)_{0^-0^-} = 2 \cos^2(Q_x X'_0) \left[\cos(Q_x X'_0) - \exp\left(-\frac{X'^2_0}{2u^2_{0x}}\right) \right]^2 \exp -Q_x^2 \left(\frac{u^2_{0x}}{2\sqrt{1+4\lambda_x}} + \frac{u^2_{0x}}{2} \right) \delta(\omega).$$

The Gaussian profiles are modulated by the $\sin^4(Q_x X'_0)$ and $\cos^4(Q_x X'_0)$ terms due to the quantum interference (see Fig. 5). The interference can be observed and the observed intensities are determined by the total scattering cross-section ($\sigma = 4\pi |b|^2 \sim 81.7$ barns) for all transitions. Maxima of intensity occur at $Q_x X'_0 = n\pi$ for $S(Q_x, \omega)_{0^+0^+}$ and at $Q_x X'_0 = (n + 1/2)\pi$ for $S(Q_x, \omega)_{0^+0^-}$.

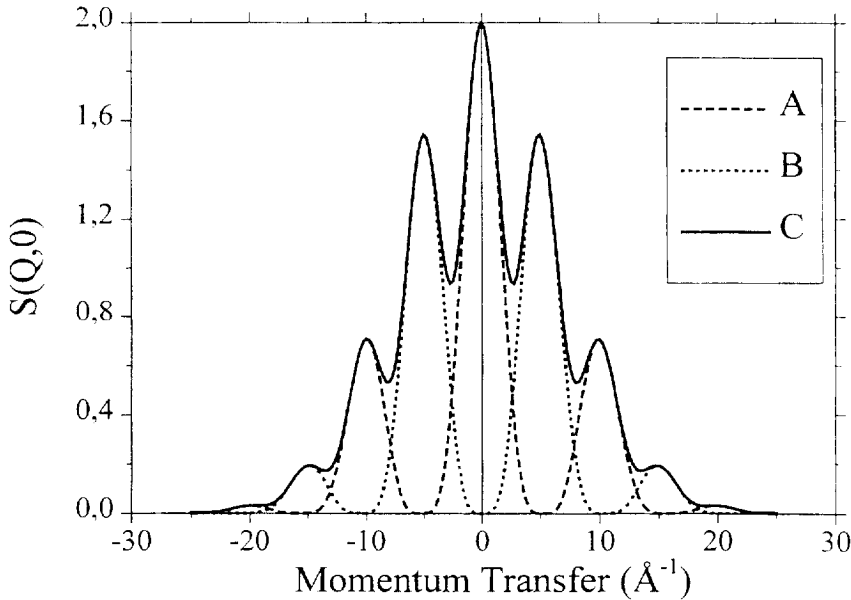


Fig. 5. Theoretical profile for elastic neutron scattering by a pair of coupled protons with spin correlation, according to Eq. (23) with $u^2_{0x} = 10^{-2} \text{ \AA}^2$ and $X'_0 = 0.3 \text{ \AA}$: (A) $S_{0^+0^+} \approx S_{0^-0^-}$; (B) $S_{0^+0^-} = S_{0^-0^+}$ and (C) total scattering function.

5. Conclusion

In the degenerate ground state, the dynamics of two coupled oscillator depends on their quantum nature. For bosons, the dynamics is represented with the usual symmetric and antisymmetric normal modes. For fermions, according to the Pauli principle spin–spin correlations give a singlet and a triplet state.

In the crystalline state the Pauli principle yields a new spin-related selection rule: in the ground state the proton (fermion) dynamics is decoupled from the dynamics of the bosons (e.g., C, O, N, ... atoms). This is in line with previous observations which revealed that decoupled dynamics is not due to accidental cancellation of the coupling terms in the force-field. In excited vibrational states, the mixing of fermion and boson coordinates is no longer forbidden. Normal coordinates can be different in the ground and excited vibrational states. This could be of importance for the calculation of intensities and force-field refinement in molecular crystals.

The calculated scattering functions for two coupled protons reveals interference effects that should be observed with elastic neutron scattering measurements. The profile is quite different from those calculated for a single proton, or a proton tunneling in a double minimum potential, or a coupled pair of bosons, or the hydrogen molecule.

The quantum effects presented in this work open up fascinating prospects for future studies. They could be of importance for a better understanding of the ordering/disordering mechanisms for protons. The quantum effects related to the Pauli principle should vanish in the deuterated crystals. Different dynamics between the protonated and deuterated crystals are not uniquely due to the mass effect.

Acknowledgements

This work was partially done while I was visiting the Department of Chemistry at the University of Otago, Dunedin, New Zealand. I am indebted to Prof. D.V. Fenby for stimulating discussions and to the University of Otago for the financial support of an Evans fellowship.

References

- [1] G.J. Keatley, F. Fillaux, M.-H. Baron, S. Bennington, J. Tomkinson, *Science* 264 (1994) 1285.
- [2] E.B. Wilson Jr., J.C. Decius, P.C. Cross, *Molecular Vibrations*, McGraw Hill, New York, 1995; P. Barchewitz, *Spectroscopie Infrarouge*, Gauthier-Villars, Paris, 1967; S.J. Cyvin, *Molecular Vibrations and Mean-Square Amplitudes*, Elsevier, Amsterdam, 1968; A.I. Kitaigorodsky, *Molecular Crystals and Molecules*, Academic Press, New York, 1973; S. Califano, V. Schettino, N. Neto, *Lattice Dynamics of Molecular Crystals*, Springer, Berlin, 1981; A.J. Pertsin, A.I. Kitaigorodsky, *The Atom–Atom Potential Method*, Springer series in Chemical Physics, Springer, Berlin, 1987.
- [3] A.C. Zemach, R.J. Glauber, *Phys. Rev.* 101 (1956) 118.
- [4] H. Jobic, J. Tomkinson, A. Renouprez, *Molecular Phys.* 39 (1980) 989.
- [5] H. Jobic, R.E. Gosh, A. Renouperz, *J. Chem. Phys.* 75 (1981) 4025.
- [6] A. Griffin, H. Jobic, *J. Chem. Phys.* 75 (1981) 5940.
- [7] H. Jobic, H. Lauter, *J. Chem. Phys.* 88 (1988) 5450.
- [8] S.W. Lovesey, *Theory of Neutron Scattered from Condensed Matter*, Vol. I: Nuclear Scattering, Clarendon Press, Oxford, 1984.
- [9] G.J. Kearley, *J. Chem. Soc. Faraday Trans. II* 82 (1986) 41.
- [10] F. Fillaux, J. Tomkinson, J. Penfold, *Chem. Phys.* 124 (1988) 425.
- [11] F. Fillaux, J.P. Fontaine, M.-H. Baron, G.J. Kearley, J. Tomkinson, *Chem. Phys.* 176 (1993) 249.
- [12] F. Fillaux, J.P. Fontaine, M.-H. Baron, N. Leygue, G.J. Kearley, J. Tomkinson, *Biophys. Chem.* 53 (1994) 155.
- [13] P. Schuster, G. Zundel, C. Sandorfy (Eds.), *The Hydrogen Bond: Recent developments in Theory and Experiments*, vols. 1–3, North-Holland, Amsterdam, 1976.
- [14] H. Ratajczak, W.J. Orville-Thomas (Eds.), *Molecular Interactions*, vol. 1, Wiley, New York, 1980.
- [15] V.A. Bendrski, D.E. Makarov, C.A. Wight, *Chemical dynamics at low temperature*, in: I. Prigogine, S.A. Rice (Eds.), *Advances in Chemical Physics*, vol. LXXXVIII, Wiley, New York, 1994.

- [16] S. Nagaoka, T. Terao, F. Imashiro, A. Saika, N. Hirota, S. Hayashi, *J. Chem. Phys.* 79 (1983) 4694; T. Agaki, F. Imashiro, T. Terao, N. Hirota, S. Hayashi, *Chem. Phys. Lett.* 139 (1987) 331; R. Meyer, R.R. Ernst, *J. Chem. Phys.* 86 (1987) 784.
- [17] J.L. Skinner, H.P. Trommsdorff, *J. Chem. Phys.* 89 (1988) 897.
- [18] A.J. Horsewill, A. Aibout, *J. Phys.: Condens. Matter* 1 (1989) 9609; A. Stäckli, B.H. Meier, R. Kreis, R. Meyer, R.R. Ernst, *J. Chem. Phys.* 93 (1990) 1502; A. Heuer, U.J. Haeberlen, *J. Chem. Phys.* 95 (1991) 4201; A.J. Horsewill, A. Heidemann, S. Hayashi, *Z. Phys. B* 90 (1993) 319; A.J. Horsewill, A. Ikram, *Physica B* 226 (1996) 202.
- [19] F. Fillaux, *Chem. Phys.* 74 (1983) 405.
- [20] P. Postorino, F. Fillaux, J. Mayers, J. Tomiksons, R.S. Holt, *J. Chem. Phys.* 94 (1991) 4411.
- [21] O. Thomas, R. Tellegren, I. Olovsson, *Acta Cryst. B* 30 (1974) 1155.
- [22] O. Thomas, R. Tellegren, I. Olovsson, *Acta Cryst. B* 30 (1974) 2540.
- [23] A. Novak, *Struct. Bonding* 18 (1974) 177.
- [24] A. Novak, P. Saumagne, L.D.C. Bock, *J. Chim. Phys.* (1963) 1385.
- [25] K. Nakamoto, Y.A. Sarma, K. Ogoshi, *J. Chem. Phys.* 43 (1965) 1177.
- [26] G. Lucazeau, A. Novak, *J. Raman Spec.* 1 (1973) 573.
- [27] F. Fillaux, A. Lautié, J. Tomkinson, G.J. Kearley, *Chem. Phys.* 154 (1991) 135; F. Fillaux, J. Tomkinson, *Chem. Phys.* 158 (1991) 113; F. Fillaux, J. Tomkinson, *J. Mol. Struct.* 270 (1992) 339.
- [28] C. Cohen-Tannoudji, B. Diu, F. Laloë, *Mécanique Quantique*, Hermann, Paris, 1977, vol. I, p. 576.